# The Elliptical Cone of Uncertainty and Its Normalized Measures in Diffusion Tensor Imaging

Cheng Guan Koay*, Uri Nevo, Lin-Ching Chang, Carlo Pierpaoli, and Peter J. Basser

***Abstract*—Diffusion tensor magnetic resonance imaging (DT-MRI) is capable of providing quantitative insights into tissue microstructure in the brain. An important piece of information offered by DT-MRI is the directional preference of diffusing water molecules within a voxel. Building upon this local directional information, DT-MRI tractography attempts to construct global connectivity of white matter tracts. The interplay between local directional information and global structural information is crucial in understanding changes in tissue microstructure as well as in white matter tracts. To this end, the right circular cone of uncertainty was proposed by Basser as a local measure of tract dispersion. Recent experimental observations by Jeong *et al.* and Lazar *et al.* that the cones of uncertainty in the brain are mostly elliptical motivate the present study to investigate analytical approaches to quantify their findings. Two analytical approaches for constructing the elliptical cone of uncertainty, based on the first-order matrix perturbation and the error propagation method via diffusion tensor representations, are presented and their theoretical equivalence is established. We propose two normalized measures, circumferential and areal, to quantify the uncertainty of the major eigenvector of the diffusion tensor. We also describe a new technique of visualizing the cone of uncertainty in 3-D.**

***Index Terms*—Cone of uncertainty, diffusion tensor imaging (DTI), eigenvector dispersion, normalized areal measure, normalized circumferential measure.**

## I. Introduction

DIFFUSION tensor magnetic resonance imaging (DT-MRI) is a noninvasive *in vivo* imaging technique uniquely capable of probing tissue microstructure in the brain [1]–[5]. DT-MRI has provided great impetus for quantifying and characterizing changes in human brain morphology [5]–[8] and in anatomical connectivity of white matter tracts [9]–[16].

Within an imaging voxel, the directional information of white matter tracts is usually obtained from the major eigenvector of the diffusion tensor [1]. Using this local directional information, DT-MRI tractography attempts to construct global anatomical connectivity of white matter tracts. The interplay between local directional and global structural information is crucial in understanding changes in white matter tracts. With this end in view, the cone of uncertainty (COU) was proposed by Basser [17] as a local measure of tract dispersion, but the shape of the cone had been presumed circular both in [17] and in later studies [18]–[24]. For example, the noninformative prior in angular space used by Behrens *et al.* [23] and the zeroth order directional uncertainty proposed by Parker *et al.* [24] were modeled after directional dispersion that is symmetric or circular. Although we have previously described an analytical method based on error propagation via diffusion tensor representations to account for asymmetry in tract dispersion [25], [47] the experimental observations by Jeong *et al.* [26] and Lazar *et al.* [27], [28] that the cones of uncertainty in the brain are mostly elliptical call for a closer investigation of analytical approaches to support their nonparametric studies, which were based on the bootstrap method. Since the dispersion is actually elliptical, the proposed analytical local measure of tract dispersion has a critical role to play in both deterministic and probabilistic methods of tractography [23], [24], [29]–[32].

To date, there are two analytical methods that can be employed to study tract dispersion—perturbation [17], [20], [29], [33], [34] and error propagation via diffusion tensor representations [25], [47]. Although Hext [33] did discuss the asymmetry of the dispersion of the eigenvector of a second order tensor, the formulation he provides, as we will show, was not suitable for practical computation and visualization because the covariance matrix of the eigenvector was not explicitly given, which might explain why it was not adopted in DT-MRI studies even though his work was made known by Anderson [29]. Furthermore, the formulation by Hext was based upon the ordinary linear least squares method, which has been shown to be less optimal than the nonlinear least squares method when applied to diffusion tensor estimation [35]–[37]. We should also remark that previous DTI studies on tract or eigenvector dispersion [17], [20], [29], [33] did not provide an explicit expression for the covariance of the eigenvector of the diffusion tensor and these studies were also based on the linear least squares method of DTI.

Based on our recent work [25], [47], we have identified the covariance matrix of the major eigenvector of the diffusion tensor as the most appropriate object for quantifying local tract dispersion. In this paper, we will reformulate the first-order matrix perturbation method used by Hext to obtain the same covariance matrix obtained in [25] and [47]. The reformulation has two very important roles—analytical as well as practical. First, as a practical construct, it renders the

Manuscript received September 11, 2007; revised November 29, 2007. This work was supported by the Intramural Research Program of the National Institute of Child Health and Human Development, National Institutes of Health, Bethesda, MD.*Asterisk indicates corresponding author.*

*C. G. Koay is with the National Institute of Child Health and Human Development, National Institutes of Health, 13 South Drive, Bethesda, MD 20892 USA (e-mail: guankoac@mail.nih.gov).

U. Nevo, C. Pierpaoli, and P. J. Basser are with the National Institute of Child Health and Human Development, National Institutes of Health, Bethesda, MD 20892 USA.

L.-C. Chang is with the National Institute of Child Health and Human Development, National Institutes of Health, Bethesda, MD 20892 USA and with the Department of Electrical Engineering and Computer Science, The Catholic University of America, Washington, DC 20064 USA.

Color versions of one or more of the figures in this paper are available online at http://ieeexplore.ieee.org.

Digital Object Identifier 10.1109/TMI.2008.915663

technique of first-order matrix perturbation more suitable for computing and visualizing the elliptical cone of uncertainty. Second, as a theoretical construct, it enables the constructive proof of the equivalence between the two covariance matrices obtained from two different approaches—the first-order matrix perturbation and the error propagation method via diffusion tensor representations.

Although the covariance matrix of the major eigenvector contains all the necessary information for constructing the elliptical COU, a normalized scalar measure of the elliptical COU may also be useful in understanding tract dispersion and in displaying uncertainties of the cones as an image. To this end, we propose two new normalized measures—the normalized circumferential and areal measures of the elliptical COU. We also propose a new approach for constructing the COU that would resolve the issue of overlapping cones in neighboring locations.

## II. Methods

### A. Review of Nonlinear Estimation of the Diffusion Tensor in Different Tensor Representations

Diffusion tensor estimation by a linear least squares method initially proposed by Basser *et al.* [1], [2] is now a routine procedure in DT-MRI studies even though recent studies [35]–[37] have shown the nonlinear least squares method to be more appropriate and accurate than the linear least squares method. Recently, we initiated a line of investigation starting from the basic properties of MR noise [38], particularly the fundamental relationship between Gaussian and Rician noise, to the methods for nonlinear estimation of the diffusion tensor [36], [37], and error propagation for DT-MRI via diffusion tensor representations [25], [47]. The common theme of our approach in these works can be characterized as nonlinear and analytical because the problem faced in each stage of this line of investigation was essentially nonlinear but analytically tractable. In brief, this line of investigation attempts to make DT-MRI more quantitative and more accessible.

Throughout this paper, we will use the same notation as employed in our previous works, [37] and [25], [47]. Although we have tried to make the present work as self-contained as possible, we should mention that it is intricately connected to the nonlinear least squares estimation of the diffusion tensor [37] and the method of error propagation via diffusion tensor representations [25], [47]. Therefore, readers are encouraged to skim through [37] and [25], [47] to get a more holistic picture of the interconnectedness of various concepts and ideas introduced here and in [25], [47], [37].

In general, the objective functions for the nonlinear least squares problem in DTI in the ordinary [37] and Euler diffusion tensor representations [25] and [47] can be expressed respectively as follows:

$$f_{\mathrm{NLS}}(\boldsymbol{\gamma}) = \frac{1}{2}\sum_{i=1}^{n}\left(\underbrace{s_i - \exp\left[\sum_{j=1}^{7} W_{ij}\gamma_j\right]}_{r_i(\boldsymbol{\gamma})}\right)^2 \tag{1}$$

and

$$f_{\mathrm{ENLS}}(\boldsymbol{\gamma}(\boldsymbol{\xi})) = \frac{1}{2}\sum_{i=1}^{n}\left(\underbrace{s_i - \exp\left[\sum_{j=1}^{7} W_{ij}\gamma_j(\boldsymbol{\xi})\right]}_{r_i(\boldsymbol{\gamma}(\boldsymbol{\xi}))}\right)^2 \tag{2}$$

and the covariance matrices of these representations are given by [25], [47]:

$$\boldsymbol{\Sigma}_{\boldsymbol{\gamma}} = \sigma_{DW}^2[\mathbf{W}^T(\hat{\mathbf{S}}^2 - \mathbf{R}\hat{\mathbf{S}})\mathbf{W}]^{-1} \tag{3}$$

and

$$\boldsymbol{\Sigma}_{\boldsymbol{\xi}} = \sigma_{DW}^2\left[\mathbf{J}_{\boldsymbol{\xi}}^T(\boldsymbol{\gamma}(\hat{\boldsymbol{\xi}}))\mathbf{W}^T(\hat{\mathbf{S}}^2 - \mathbf{R}\hat{\mathbf{S}})\mathbf{W}\mathbf{J}_{\boldsymbol{\xi}}(\boldsymbol{\gamma}(\hat{\boldsymbol{\xi}}))\right]^{-1}. \tag{4}$$

The matrix or vector transposition is denoted by superscript $T$. The notations used in (1)–(4) are defined in Appendix I.

### B. Error Propagation Framework

The core idea of error propagation is to transform one covariance matrix to another covariance matrix of interest through an appropriate mapping between the underlying representations [25], [47].

In DT-MRI, the most fundamental covariance matrix is $\boldsymbol{\Sigma}_{\boldsymbol{\gamma}}$, from which other covariance matrices can be obtained [25], [47]. For example, $\boldsymbol{\Sigma}_{\boldsymbol{\xi}}$ can be constructed from $\boldsymbol{\Sigma}_{\boldsymbol{\gamma}}$ as follows:

$$\boldsymbol{\Sigma}_{\boldsymbol{\xi}} = \mathbf{J}_{\boldsymbol{\gamma}}(\boldsymbol{\xi}(\hat{\boldsymbol{\gamma}}))\boldsymbol{\Sigma}_{\boldsymbol{\gamma}}\mathbf{J}_{\boldsymbol{\gamma}}^T(\boldsymbol{\xi}(\hat{\boldsymbol{\gamma}})) \tag{5}$$

where $\mathbf{J}_{\boldsymbol{\gamma}}(\boldsymbol{\xi}(\hat{\boldsymbol{\gamma}}))$, $[\mathbf{J}_{\boldsymbol{\gamma}}(\boldsymbol{\xi}(\hat{\boldsymbol{\gamma}}))]_{ij} \equiv \partial\xi_i(\boldsymbol{\gamma})/\partial\gamma_j|_{\boldsymbol{\gamma}=\hat{\boldsymbol{\gamma}}}$, is known as the Jacobian matrix of $\boldsymbol{\xi}$ with respect to $\boldsymbol{\gamma}$ evaluated at $\hat{\boldsymbol{\gamma}}$. This Jacobian matrix is a locally linear map from $d\boldsymbol{\gamma}$ to $d\boldsymbol{\xi}$ at $\hat{\boldsymbol{\gamma}}$, e.g.,

$$d\boldsymbol{\xi} = \mathbf{J}_{\boldsymbol{\gamma}}(\boldsymbol{\xi}(\hat{\boldsymbol{\gamma}}))\, d\boldsymbol{\gamma}. \tag{6}$$

In general, an explicit mapping, i.e., $\boldsymbol{\xi}(\boldsymbol{\gamma})$, is needed to reconstruct the Jacobian matrix, i.e., $\mathbf{J}_{\boldsymbol{\gamma}}(\boldsymbol{\xi})$; although $\boldsymbol{\xi}(\boldsymbol{\gamma})$ exists [39], it is neither accurate computationally compared to matrix diagonalization nor useful conceptually. To drive home this point, the reader is invited to derive the analytical expression of $\partial\xi_i/\partial\gamma_j$. The Euler representation was therefore proposed [25], [47] to resolve this issue by expressing the ordinary tensor representation in terms of the Euler representation, $\boldsymbol{\gamma}(\boldsymbol{\xi})$; this mapping is related to the decomposition of a symmetric matrix. As a confirmation that these two formulations are indeed equivalent *in principle*, we will derive (4) by substituting (3) into (5)

$$\begin{aligned}
\boldsymbol{\Sigma}_{\boldsymbol{\xi}} &= \mathbf{J}_{\boldsymbol{\gamma}}(\boldsymbol{\xi}(\hat{\boldsymbol{\gamma}}))\,\boldsymbol{\Sigma}_{\boldsymbol{\gamma}}\mathbf{J}_{\boldsymbol{\gamma}}^T(\boldsymbol{\xi}(\hat{\boldsymbol{\gamma}})) \\
&= \sigma_{DW}^2\mathbf{J}_{\boldsymbol{\gamma}}(\boldsymbol{\xi}(\hat{\boldsymbol{\gamma}}))\,[\mathbf{W}^T(\hat{\mathbf{S}}^2 - \mathbf{R}\hat{\mathbf{S}})\mathbf{W}]^{-1}\mathbf{J}_{\boldsymbol{\gamma}}^T(\boldsymbol{\xi}(\hat{\boldsymbol{\gamma}})) \\
&= \sigma_{DW}^2\left(\mathbf{J}_{\boldsymbol{\gamma}}(\boldsymbol{\xi}(\hat{\boldsymbol{\gamma}}))\right)^{(-1)(-1)} \\
&\quad \times [\mathbf{W}^T(\hat{\mathbf{S}}^2 - \mathbf{R}\hat{\mathbf{S}})\mathbf{W}]^{-1}\left(\mathbf{J}_{\boldsymbol{\gamma}}^T(\boldsymbol{\xi}(\hat{\boldsymbol{\gamma}}))\right)^{(-1)(-1)} \\
&= \sigma_{DW}^2\left[\left(\mathbf{J}_{\boldsymbol{\gamma}}^T(\boldsymbol{\xi}(\hat{\boldsymbol{\gamma}}))\right)^{-1}(\mathbf{W}^T(\hat{\mathbf{S}}^2 - \mathbf{R}\hat{\mathbf{S}})\mathbf{W}\right. \\
&\quad \left.\times\left(\mathbf{J}_{\boldsymbol{\gamma}}(\boldsymbol{\xi}(\hat{\boldsymbol{\gamma}}))\right)^{-1}\right]^{-1} \\
&= \sigma_{DW}^2\left[\mathbf{J}_{\boldsymbol{\xi}}^T(\boldsymbol{\gamma}(\hat{\boldsymbol{\xi}}))\,\mathbf{W}^T(\hat{\mathbf{S}}^2 - \mathbf{R}\hat{\mathbf{S}})\mathbf{W}\mathbf{J}_{\boldsymbol{\xi}}(\boldsymbol{\gamma}(\hat{\boldsymbol{\xi}}))\right]^{-1}.
\end{aligned}$$

In the above derivation, we used the following well-known identity $\mathbf{J}_{\boldsymbol{\xi}}(\boldsymbol{\gamma}(\hat{\boldsymbol{\xi}})) \cdot \mathbf{J}_{\boldsymbol{\gamma}}(\boldsymbol{\xi}(\hat{\boldsymbol{\gamma}})) = \mathbf{J}_{\boldsymbol{\xi}}(\boldsymbol{\xi}(\hat{\boldsymbol{\xi}})) = \mathbf{I}$, and, therefore, $[\mathbf{J}_{\boldsymbol{\gamma}}(\boldsymbol{\xi}(\hat{\boldsymbol{\gamma}}))]^{-1} = \mathbf{J}_{\boldsymbol{\xi}}(\boldsymbol{\gamma}(\hat{\boldsymbol{\xi}}))$. In practice, it is easier to compute $\mathbf{J}_{\boldsymbol{\xi}}(\boldsymbol{\gamma}(\hat{\boldsymbol{\xi}}))$ than $\mathbf{J}_{\boldsymbol{\gamma}}(\boldsymbol{\xi}(\hat{\boldsymbol{\gamma}}))$. This seemingly trivial technique of transforming one problem to another in which the Jacobian matrix of the latter has a much simpler expression will be exploited again later.

As can be seen above, the Jacobian matrix between representations plays a critical role in transforming one covariance matrix to another and the Jacobian matrix is, in turn, dependent upon the mapping between representations. In light of this understanding, we will reformulate the perturbation method in the next section to elucidate how the Jacobian matrix between the ordinary representation and the major eigenvector can be constructed so that the covariance matrix of the major eigenvector can be obtained.

We should note that an explicit mapping between representations is usually needed to construct the Jacobian matrix. Occasionally, such a mapping may not exist or may be too complicated to shed light on the problem at hand. If this is the case then the first-order matrix perturbation method may be helpful in finding the Jacobian matrix in the form of $d\boldsymbol{\xi} = \mathbf{J}_{\boldsymbol{\gamma}}(\boldsymbol{\xi}(\hat{\boldsymbol{\gamma}}))d\boldsymbol{\gamma}$ without requiring an explicit mapping of $\boldsymbol{\xi}(\boldsymbol{\gamma})$.

### C. First-Order Matrix Perturbation Method Reformulated

The first comprehensive theoretical analysis of noise in DT-MRI via the method of matrix perturbation was carried out by Anderson [29], and since then, many studies have built upon this work in understanding tract dispersion [27], [30] and variability in scalar tensor-derived quantities [20]. Further, it is through this work that we learned of the work by Hext [33] in which the local dispersion of the major eigenvector was first formulated. This formulation of local dispersion is different from that of Basser [17] because the latter leads to a circular cone of uncertainty. It is important to note that the covariance matrix of the second order tensor used by Hext [33], Anderson [29], Basser *et al.* [17], and Chang *et al.* [20] was based on the linear least squares methods, ordinary, or weighted. In this work, the covariance matrix of the diffusion tensor is based on the nonlinear least squares method, which is consistent with our previous works [25], [47], [37].

We will introduce a notation, $\mathbf{a}(\cdot,\cdot)$, used by Hext [33] to simplify our discussion. Let

$$\mathbf{Q} = \begin{pmatrix} Q_{11} & Q_{12} & Q_{13} \\ Q_{21} & Q_{22} & Q_{23} \\ Q_{31} & Q_{32} & Q_{33} \end{pmatrix}$$

$$\mathbf{q}_1 = \begin{pmatrix} q_{1x} \\ q_{1y} \\ q_{1z} \end{pmatrix} = \begin{pmatrix} Q_{11} \\ Q_{21} \\ Q_{31} \end{pmatrix}$$

$$\mathbf{q}_2 = \begin{pmatrix} q_{2x} \\ q_{2y} \\ q_{2z} \end{pmatrix} = \begin{pmatrix} Q_{12} \\ Q_{22} \\ Q_{32} \end{pmatrix}$$

and

$$\mathbf{q}_3 = \begin{pmatrix} q_{3x} \\ q_{3y} \\ q_{3z} \end{pmatrix} = \begin{pmatrix} Q_{13} \\ Q_{23} \\ Q_{33} \end{pmatrix}$$

we can write the quadratic form, $\mathbf{q}_i^T \cdot \mathbf{D} \cdot \mathbf{q}_j$, as a dot product between two vectors as follows, which is a well known trick in DT-MRI:

$$\mathbf{q}_i^T \cdot \mathbf{D} \cdot \mathbf{q}_j = \mathbf{a}(\mathbf{q}_i, \mathbf{q}_j)^T \cdot \boldsymbol{\beta} \tag{7}$$

where

$$\begin{aligned} &\mathbf{a}(\mathbf{q}_i, \mathbf{q}_j)^T \\ &\quad \equiv [q_{ix}q_{jx},\ q_{iy}q_{jy}, q_{iz}q_{jz}, q_{ix}q_{jy} + q_{iy}q_{jx} \\ &\qquad q_{iy}q_{jz} + q_{iz}q_{jy}, q_{ix}q_{jz} + q_{iz}q_{jx}] \end{aligned} \tag{8}$$

is the notation used by Hext, and

$$\boldsymbol{\beta} \equiv [D_{xx},\ D_{yy},\ D_{zz},\ D_{xy},\ D_{yz},\ D_{xz}]^T. \tag{9}$$

The first-order matrix perturbation method begins with the eigenvalue equation and the orthonormality condition

$$\mathbf{D} \cdot \mathbf{q}_i = \lambda_i \mathbf{q}_i \tag{10}$$

and

$$\mathbf{q}_i^T \mathbf{q}_j = \delta_{ij} \tag{11}$$

respectively. Here, $\delta_{ij}$ is the Kronecker delta function, which assumes unity if $i = j$ or zero otherwise.

If we take a small variation on both sides of (10), i.e., $\delta(\mathbf{D} \cdot \mathbf{q}_i) = \delta(\lambda_i \mathbf{q}_i)$, and of (11), i.e., $\delta(\mathbf{q}_i^T \mathbf{q}_j) = \delta(\delta_{ij})$, the former leads to

$$\delta\mathbf{D} \cdot \mathbf{q}_i + \mathbf{D} \cdot \delta\mathbf{q}_i = \delta\lambda_i\, \mathbf{q}_i + \lambda_i\, \delta\mathbf{q}_i \tag{12}$$

while the latter leads to

$$\delta\mathbf{q}_i^T \cdot \mathbf{q}_j + \mathbf{q}_i^T \cdot \delta\mathbf{q}_j = \delta(\delta_{ij}) = 0 \quad \text{for } i, j = 1, 2, 3. \tag{13}$$

Equation (13) also implies that

$$\delta\mathbf{q}_i^T \cdot \mathbf{q}_j = -\mathbf{q}_i^T \cdot \delta\mathbf{q}_j \quad \text{for } i \neq j \tag{14}$$

and from $\mathbf{q}_i^T \mathbf{q}_i = 1$ we obtain

$$\mathbf{q}_i^T \cdot \delta\mathbf{q}_i = 0 \quad \text{or} \quad \delta\mathbf{q}_i^T \cdot \mathbf{q}_i = 0 \quad \text{for } i = 1, 2, 3. \tag{15}$$

Taking the dot product between (12) with $\mathbf{q}_j^T$, we have

$$\mathbf{q}_j^T \cdot \delta\mathbf{D} \cdot \mathbf{q}_i + \mathbf{q}_j^T \cdot \mathbf{D} \cdot \delta\mathbf{q}_i = \delta\lambda_i \underbrace{\mathbf{q}_j^T \cdot \mathbf{q}_i}_{0} + \lambda_i\, \mathbf{q}_j^T \cdot \delta\mathbf{q}_i$$

$$\mathbf{q}_j^T \cdot \delta\mathbf{D} \cdot \mathbf{q}_i + (\mathbf{D}^T \cdot \mathbf{q}_j)^T \cdot \delta\mathbf{q}_i = \lambda_i\, \mathbf{q}_j^T \cdot \delta\mathbf{q}_i. \tag{16}$$

Since $\mathbf{D}$ is symmetric, (16) can be further reduced to the following expression by taking (10) into account:

$$\mathbf{q}_j^T \cdot \delta\mathbf{D} \cdot \mathbf{q}_i + \lambda_j \cdot \mathbf{q}_j^T \cdot \delta\mathbf{q}_i = \lambda_i\, \mathbf{q}_j^T \cdot \delta\mathbf{q}_i \tag{17}$$

$$\mathbf{q}_j^T \cdot \delta\mathbf{q}_i = \frac{1}{(\lambda_i - \lambda_j)} \mathbf{q}_j^T \cdot \delta\mathbf{D} \cdot \mathbf{q}_i$$
$$\mathbf{q}_j^T \cdot \delta\mathbf{q}_i = \frac{1}{(\lambda_i - \lambda_j)} \mathbf{a}(\mathbf{q}_j, \mathbf{q}_i)^T \cdot \delta\boldsymbol{\beta}. \quad (18)$$

The derivation thus far can be found in Hext [33]. In order to obtain the covariance structure of the major vector of the diffusion tensor, we should keep in mind one of the key objects in error propagation, namely, the Jacobian matrix between representations in a form similar to (6). Although (18) differs slightly from (6), we will reformulate it to achieve the desired form of $\delta\mathbf{q}_i = \mathbf{J}_{\boldsymbol{\beta}}(\mathbf{q}_i)\delta\boldsymbol{\beta}$. Later, we will extend the reformulation from $\delta\mathbf{q}_i = \mathbf{J}_{\boldsymbol{\beta}}(\mathbf{q}_i)\delta\boldsymbol{\beta}$ to $\delta\mathbf{q}_i = \mathbf{J}_{\boldsymbol{\gamma}}(\mathbf{q}_i)\delta\boldsymbol{\gamma}$.

Without loss of generality, we assume that $\lambda_1 > \lambda_2 > \lambda_3$. Since we are interested in the dispersion of the major eigenvector, we will take $i = 1$. We should point out that the dispersion of the medium and minor eigenvectors can be similarly derived. Note that (18) results in three separate equations, namely

$$\mathbf{q}_1^T \cdot \delta\mathbf{q}_1 = [0,0,0,0,0,0] \cdot \delta\boldsymbol{\beta} \quad (19)$$
$$\mathbf{q}_2^T \cdot \delta\mathbf{q}_1 = \frac{1}{(\lambda_1 - \lambda_2)} \mathbf{a}(\mathbf{q}_2, \mathbf{q}_1)^T \cdot \delta\boldsymbol{\beta} \quad (20)$$

and

$$\mathbf{q}_3^T \cdot \delta\mathbf{q}_1 = \frac{1}{(\lambda_1 - \lambda_3)} \mathbf{a}(\mathbf{q}_3, \mathbf{q}_1)^T \cdot \delta\boldsymbol{\beta}. \quad (21)$$

Note that (19) is a consequence of (15) and not of (17). Equations (19)–(21) can be combined into a single matrix expression given by

$$\underbrace{\begin{pmatrix} \mathbf{q}_1^T \\ \mathbf{q}_2^T \\ \mathbf{q}_3^T \end{pmatrix}}_{\mathbf{Q}^T} \cdot \delta\mathbf{q}_1 = \underbrace{\begin{pmatrix} 0 & 0 & 0 & 0 & 0 & 0 \\ \frac{1}{(\lambda_1-\lambda_2)}\mathbf{a}(\mathbf{q}_2,\mathbf{q}_1)^T \\ \frac{1}{(\lambda_1-\lambda_3)}\mathbf{a}(\mathbf{q}_3,\mathbf{q}_1)^T \end{pmatrix}}_{\mathbf{S}_1} \cdot \delta\boldsymbol{\beta}$$

which is $\mathbf{Q}^T \cdot \delta\mathbf{q}_1 = \mathbf{S}_1 \cdot \delta\boldsymbol{\beta}$, or

$$\delta\mathbf{q}_1 = \mathbf{Q} \cdot \mathbf{S}_1 \cdot \delta\boldsymbol{\beta}. \quad (22)$$

In the above derivation, we have used the orthonormality condition, i.e., $\mathbf{Q}\mathbf{Q}^T = \mathbf{I}$.

The above reformulation based on $\boldsymbol{\beta}$ can be easily extended to $\boldsymbol{\gamma}$ resulting in

$$\delta\mathbf{q}_1 = \mathbf{Q} \cdot \mathbf{T}_1 \cdot \delta\boldsymbol{\gamma} \quad (23)$$

where $\mathbf{T}_1$ is a $3 \times 7$ matrix given by

$$\begin{pmatrix} 0 & 0 & 0 & 0 & 0 & 0 & 0 \\ 0 & \frac{1}{(\lambda_1-\lambda_2)}\mathbf{a}(\mathbf{q}_2,\mathbf{q}_1)^T \\ 0 & \frac{1}{(\lambda_1-\lambda_3)}\mathbf{a}(\mathbf{q}_3,\mathbf{q}_1)^T \end{pmatrix}.$$

Therefore, we have $\mathbf{Q}\mathbf{S}_1 = \mathbf{J}_{\boldsymbol{\beta}}(\mathbf{q}_1)$ and $\mathbf{Q}\mathbf{T}_1 = \mathbf{J}_{\boldsymbol{\gamma}}(\mathbf{q}_1)$.

Finally, the covariance of the major eigenvector can be expressed nicely as [25], [47]

$$\boldsymbol{\Sigma}_{\mathbf{q}_1}(\hat{\boldsymbol{\gamma}}) = \mathbf{J}_{\boldsymbol{\gamma}}(\mathbf{q}_1)\, \boldsymbol{\Sigma}_{\boldsymbol{\gamma}}(\hat{\boldsymbol{\gamma}})\, \mathbf{J}_{\boldsymbol{\gamma}}^T(\mathbf{q}_1). \quad (24)$$

Interestingly, the formulation used by Basser [17] or Fukunaga [34] and later by Chang *et al.* [20] can be deduced from the present framework starting from (22)

$$\delta\mathbf{q}_1 = \mathbf{Q} \cdot \mathbf{S}_1 \cdot \delta\boldsymbol{\beta},$$
$$\delta\mathbf{q}_1 = (\mathbf{q}_1 \quad \mathbf{q}_2 \quad \mathbf{q}_3) \cdot \begin{pmatrix} 0 \\ \frac{1}{(\lambda_1-\lambda_2)}\mathbf{a}(\mathbf{q}_2,\mathbf{q}_1)^T \cdot \delta\boldsymbol{\beta} \\ \frac{1}{(\lambda_1-\lambda_3)}\mathbf{a}(\mathbf{q}_3,\mathbf{q}_1)^T \cdot \delta\boldsymbol{\beta} \end{pmatrix}$$

or

$$\delta\mathbf{q}_1 = 0\,\mathbf{q}_1 + \left(\frac{1}{(\lambda_1 - \lambda_2)}\mathbf{a}(\mathbf{q}_2, \mathbf{q}_1)^T \cdot \delta\boldsymbol{\beta}\right)\mathbf{q}_2 + \left(\frac{1}{(\lambda_1 - \lambda_3)}\mathbf{a}(\mathbf{q}_3, \mathbf{q}_1)^T \cdot \delta\boldsymbol{\beta}\right)\mathbf{q}_3$$

so that

$$\delta\mathbf{q}_1 = \left(\frac{\mathbf{q}_2^T \cdot \delta\mathbf{D} \cdot \mathbf{q}_1}{(\lambda_1 - \lambda_2)}\right)\mathbf{q}_2 + \left(\frac{\mathbf{q}_3^T \cdot \delta\mathbf{D} \cdot \mathbf{q}_1}{(\lambda_1 - \lambda_3)}\right)\mathbf{q}_3. \quad (25)$$

In retrospect, it may seem trivial that (22) can be deduced from (25). Although such a derivation is short, it may seem too artificial without sufficient motivation on the crucial role played by the Jacobian matrix in error propagation. Furthermore, the covariance of the major eigenvector as a geometric structure for quantifying local tract dispersion is a concept that was introduced only recently [25], [47]. From (25), we see that the vector, $\delta\mathbf{q}_1$, is perpendicular to the major eigenvector, $\mathbf{q}_1$, because $\delta\mathbf{q}_1$ is a linear combination of $\mathbf{q}_2$ and $\mathbf{q}_3$. For completeness, we provide the expression for the angle of deviation of the right circular cone of uncertainty [17], [20]

$$\theta_C = \tan^{-1}(\|\delta\mathbf{q}_1\|/\|\mathbf{q}_1\|) = \tan^{-1}(\|\delta\mathbf{q}_1\|)$$
$$= \tan^{-1}\left(\sqrt{\left(\frac{\mathbf{q}_2^T \cdot \delta\mathbf{D} \cdot \mathbf{q}_1}{(\lambda_1 - \lambda_2)}\right)^2 + \left(\frac{\mathbf{q}_3^T \cdot \delta\mathbf{D} \cdot \mathbf{q}_1}{(\lambda_1 - \lambda_3)}\right)^2}\right). \quad (26)$$

Note that $\delta\mathbf{D}$ is taken to be the standard deviation of the tensor elements in computing the angle in (26), [17], [20], [29].

As mentioned above, an explicit mapping between representations may not be available as is the case between $\mathbf{q}_1$ and $\boldsymbol{\gamma}$ but $\delta\mathbf{q}_1 = \mathbf{Q} \cdot \mathbf{T}_1 \cdot \delta\boldsymbol{\gamma}$ can still be computed.

In concluding this section, we will demonstrate that (24) can be derived from the approach proposed in [25], [47]. The covariance of the major eigenvector of the diffusion tensor using the Euler representation is given by [25] and [47]

$$\boldsymbol{\Sigma}_{\mathbf{q}_1} = \mathbf{J}_{\hat{\boldsymbol{\xi}}}(\mathbf{q}_1(\hat{\boldsymbol{\xi}}))\, \boldsymbol{\Sigma}_{\boldsymbol{\xi}}\, \mathbf{J}_{\hat{\boldsymbol{\xi}}}^T(\mathbf{q}_1(\hat{\boldsymbol{\xi}})). \quad (27)$$

Substituting (4) into (27), we have

$$\boldsymbol{\Sigma}_{\mathbf{q}_1} = \sigma_{DW}^2 \mathbf{J}_{\boldsymbol{\xi}}(\mathbf{q}_1(\hat{\boldsymbol{\xi}})) \times \left[\mathbf{J}_{\boldsymbol{\xi}}^T(\boldsymbol{\gamma}(\hat{\boldsymbol{\xi}}))\mathbf{W}^T(\hat{\mathbf{S}}^2 - \mathbf{R}\hat{\mathbf{S}})\mathbf{W}\mathbf{J}_{\boldsymbol{\xi}}(\boldsymbol{\gamma}(\hat{\boldsymbol{\xi}}))\right]^{-1} \times \mathbf{J}_{\boldsymbol{\xi}}^T(\mathbf{q}_1(\hat{\boldsymbol{\xi}})) = \mathbf{J}_{\boldsymbol{\xi}}(\mathbf{q}_1(\hat{\boldsymbol{\xi}}))\, [\mathbf{J}_{\boldsymbol{\xi}}(\boldsymbol{\gamma}(\hat{\boldsymbol{\xi}}))]^{-1}$$

$$\times \underbrace{\sigma_{DW}^2[\mathbf{W}^T(\hat{\mathbf{S}}^2 - \mathbf{R}\hat{\mathbf{S}})\mathbf{W}]^{-1}}_{\boldsymbol{\Sigma}_\gamma} \left[\mathbf{J}_{\boldsymbol{\xi}}^T(\boldsymbol{\gamma}(\hat{\boldsymbol{\xi}}))\right]^{-1}$$
$$\times \mathbf{J}_{\boldsymbol{\xi}}^T(\mathbf{q}_1(\hat{\boldsymbol{\xi}}))$$
$$= \mathbf{J}_{\boldsymbol{\xi}}(\mathbf{q}_1(\hat{\boldsymbol{\xi}}))\,\mathbf{J}_{\boldsymbol{\gamma}}(\boldsymbol{\xi}(\hat{\boldsymbol{\gamma}}))\boldsymbol{\Sigma}_{\boldsymbol{\gamma}}\mathbf{J}_{\boldsymbol{\gamma}}^T(\boldsymbol{\xi}(\hat{\boldsymbol{\gamma}}))\mathbf{J}_{\boldsymbol{\xi}}^T(\mathbf{q}_1(\hat{\boldsymbol{\xi}}))$$
$$= \mathbf{J}_{\boldsymbol{\gamma}}(\mathbf{q}_1(\hat{\boldsymbol{\gamma}}))\boldsymbol{\Sigma}_{\boldsymbol{\gamma}}\mathbf{J}_{\boldsymbol{\gamma}}^T(\mathbf{q}_1(\hat{\boldsymbol{\gamma}})). \quad (28)$$

Two important identities were used in the derivation above: $\mathbf{J}_{\boldsymbol{\xi}}(\mathbf{q}_1(\hat{\boldsymbol{\xi}}))\mathbf{J}_{\boldsymbol{\gamma}}(\boldsymbol{\xi}(\hat{\boldsymbol{\gamma}})) = \mathbf{J}_{\boldsymbol{\gamma}}(\mathbf{q}_1(\hat{\boldsymbol{\gamma}}))$, and $[\mathbf{J}_{\boldsymbol{\xi}}(\boldsymbol{\gamma}(\hat{\boldsymbol{\xi}}))]^{-1} = \mathbf{J}_{\boldsymbol{\gamma}}(\boldsymbol{\xi}(\hat{\boldsymbol{\gamma}}))$. Although the derivation above shows that (28) can be obtained from (27), it is important to point out that it shows only the existence of $\mathbf{J}_{\boldsymbol{\gamma}}(\mathbf{q}_1(\hat{\boldsymbol{\gamma}}))$ but not necessarily the construction of $\mathbf{J}_{\boldsymbol{\gamma}}(\mathbf{q}_1(\hat{\boldsymbol{\gamma}}))$. Fortunately, as we have seen in this section, we know of one such construction.

For completeness, we will outline the steps needed to construct the cone of uncertainty following the approach used by Hext. From (28), we know that the $1-\alpha$ joint confidence region for $\mathbf{q}_1$ is the ellipsoid [40] given by

$$(\mathbf{q}_1 - \mathbf{q}_1(\hat{\boldsymbol{\gamma}}))^T\boldsymbol{\Sigma}_{\mathbf{q}_1}^{+}(\hat{\boldsymbol{\gamma}})(\mathbf{q}_1 - \mathbf{q}_1(\hat{\boldsymbol{\gamma}})) \le 2F(2, n-7;\alpha)$$

where $F(2, n-7;\alpha)$ is the upper $\alpha$ quantile for an $F$ distribution with 2 and $n-7$ degrees-of-freedom; the plus sign on $\boldsymbol{\Sigma}_{\mathbf{q}_1}^{+}$ denotes the matrix pseudoinverse which is needed here because the matrix rank of $\boldsymbol{\Sigma}_{\mathbf{q}_1}$ is two rather than three. Equivalently, one can write

$$(\mathbf{q}_1 - \mathbf{q}_1(\hat{\boldsymbol{\gamma}}))^T(2\mathcal{F}(2, n-7;\alpha)\,\boldsymbol{\Sigma}_{\mathbf{q}_1}(\hat{\boldsymbol{\gamma}}))^{+}(\mathbf{q}_1 - \mathbf{q}_1(\hat{\boldsymbol{\gamma}})) \le 1$$

and finally $\mathbf{q}_1^T(2\mathcal{F}(2, n-7;\alpha)\,\boldsymbol{\Sigma}_{\mathbf{q}_1}(\hat{\boldsymbol{\gamma}}))^{+}\mathbf{q}_1 \le 1$ because the eigenvectors of the diffusion tensor are orthogonal and the eigenvectors of $\boldsymbol{\Sigma}_{\mathbf{q}_1}(\hat{\boldsymbol{\gamma}})$ are also the singular vectors [41]. Let the eigenvalue decomposition of $\boldsymbol{\Sigma}_{\mathbf{q}_1}(\hat{\boldsymbol{\gamma}})$ be $\omega_1\mathbf{c}_1\mathbf{c}_1^T + \omega_2\mathbf{c}_2\mathbf{c}_2^T + 0\,\mathbf{q}_1(\hat{\boldsymbol{\gamma}})\,\mathbf{q}_1^T(\hat{\boldsymbol{\gamma}})$; the last term is due to $\mathbf{Q}\cdot\mathbf{T}_1 = \mathbf{J}_{\boldsymbol{\gamma}}(\mathbf{q}_1)$ and (24). Then, choosing $\mathbf{q}_1$ to be $\sqrt{2\mathcal{F}(2, n-7;\alpha)\,\omega_1}\mathbf{c}_1$ or $\sqrt{2\mathcal{F}(2, n-7;\alpha)\,\omega_2}\mathbf{c}_2$ will give us the principal directions of the ellipse of the COU whose area corresponds to the $1-\alpha$ joint confidence region for $\mathbf{q}_1$. Note that $\mathcal{F}(2, n-7;\alpha)$ can be found by solving for the root of $\alpha - I_{(n-7)/(n-7+2F)}((n-7)/2,\,1) = 0$ where $I_x(a,b)$ is the incomplete Beta function [42]. We should also mention that the covariance matrix of the major eigenvector may also be obtained from the average dyadics of the bootstrap estimates of the major eigenvector as described in [25, Appendix X] and [47].

### *D. COU Visualization and Normalized Circumferential and Areal Measures*

We propose here a technique of COU construction for visualization and two normalized measures for quantifying uncertainty in the major vector of the diffusion tensor. We will provide detailed information on the new construction of COU as well as the computation of the normalized measures in this section.

A simple closed or Jordan curve [43] on the unit sphere divides the unit sphere into two regions. If the simple closed curve is not the great circle then one region will be greater than the other. The proposed normalized areal measure, denoted by $\Gamma$, is the ratio of the area of the smaller region on the unit sphere, which is enclosed by a simple closed curve whose Gnomonic (or central) projection [44] on the $u,v$-plane is an ellipse as depicted in Fig. 1 and Fig. 2(A), to the area of the hemisphere. The ratio of the circumference of the simple closed curve on the unit sphere to the circumference of the great circle of the unit sphere is another normalized measure, denoted by $\Lambda$, that is related to the cone of uncertainty. As a spin-off of making these normalized measures practical for computation, we have a technique of constructing the COU, depicted in Fig. 2(B), that avoids overlapping cones in neighboring regions.

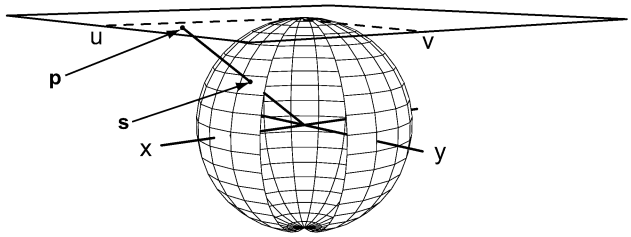


Fig. 1. Gnomonic (or central) projection.

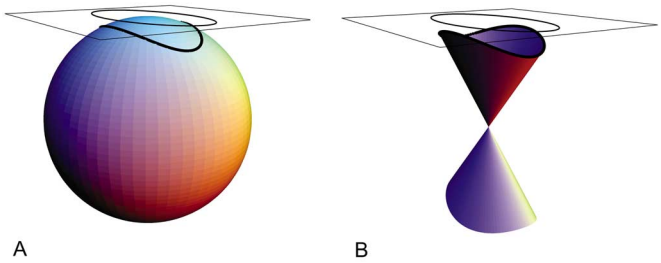


Fig. 2. (A) Inverse Gnomonic projection of an ellipse of the u,v-plane onto the unit sphere is accomplished by normalizing the vector $\mathbf{p}$ in Fig. 1 to unit length so that the normalized vector is $\mathbf{s}$. (B) The proposed construction of the COU is based on the inverse Gnomonic projection of an ellipse of the u,v-plane onto the unit sphere.

Let $\mathbf{s}$ be a point on the upper hemisphere whose Gnomonic projection on the $u,v$-plane is the point $\mathbf{p}$, Fig. 1. Let $\mathbf{p}$ be denoted in vector form by

$$\mathbf{p} = [u, v, 1]^T. \quad (29)$$

The point $\mathbf{s}$ in vector form can be obtained by normalizing $\mathbf{p}$ to unit length

$$\mathbf{s} \equiv \begin{pmatrix} X_s \\ Y_s \\ Z_s \end{pmatrix} = \frac{\mathbf{p}}{\sqrt{\mathbf{p}^T\cdot\mathbf{p}}} = \begin{pmatrix} \frac{u}{\sqrt{u^2+v^2+1}} \\ \frac{v}{\sqrt{u^2+v^2+1}} \\ \frac{1}{\sqrt{u^2+v^2+1}} \end{pmatrix}. \quad (30)$$

Therefore, the components of $\mathbf{s}$ are functions of $u$ and $v$.

Suppose that the major and the minor axes of the ellipse coincide with the axes of the $u,v$-plane. Let the length of the major and the minor axes be $a$ and $b$, respectively. Specifically, we have $a = \sqrt{2F(2, n-7;\alpha)\,\omega_1}$ and $b = \sqrt{2F(2, n-7;\alpha)\,\omega_2}$ which are taken from the previous section. The normalized areal measure, $\Gamma$, which is a dimensionless quantity, with values ranging from zero to unity can then be expressed as follows:

$$\Gamma = \frac{1}{2\pi}\iint_R \sqrt{EG - F^2}\,du\,dv \quad (31)$$

in terms of the coefficients of the first fundamental form [45]; the region $R$ is defined by $(u/a)^2+(v/b)^2 \leq 1$ and the coefficients of the first fundamental form are

$$E = (\partial X_s/\partial u)^2 + (\partial Y_s/\partial u)^2 + (\partial Z_s/\partial u)^2$$
$$G = (\partial X_s/\partial v)^2 + (\partial Y_s/\partial v)^2 + (\partial Z_s/\partial v)^2$$

and

$$F = \frac{\partial X_s}{\partial u}\frac{\partial X_s}{\partial v} + \frac{\partial Y_s}{\partial u}\frac{\partial Y_s}{\partial v} + \frac{\partial Z_s}{\partial u}\frac{\partial Z_s}{\partial v}.$$

The surface integral above can be further simplified to show explicit dependence on $a$ and $b$

$$\Gamma = \frac{2a}{\pi b\sqrt{1+a^2}} \times \left[(1+b^2)\Pi\left(-b^2, \frac{a^2-b^2}{1+a^2}\right) - \mathrm{K}\left(\frac{a^2-b^2}{1+a^2}\right)\right] \quad (32)$$

where K and $\Pi$ are, respectively, the complete elliptic integrals of the first kind and the third kind [46], which are defined below for completeness

$$\mathrm{K}(m) = \int_0^{\pi/2} \frac{1}{\sqrt{1-m\sin^2\theta}}d\theta = \int_0^1 \frac{1}{\sqrt{(1-v^2)(1-mv^2)}}dv$$

and

$$\Pi(n,m) = \int_0^{\pi/2} \frac{1}{(1-n\sin^2\theta)\sqrt{1-m\sin^2\theta}}d\theta = \int_0^1 \frac{1}{(1-nv^2)\sqrt{(1-v^2)(1-mv^2)}}dv.$$

The derivation of (32) is provided in Appendix II.

It is interesting to note the special case which occurs when the ellipse on the u,v-plane becomes a circle where $r \equiv a = b$. In this case, the normalized areal measure is given by

$$\Gamma = 1 - \frac{1}{\sqrt{1+r^2}}. \quad (33)$$

The derivation of (33) involves a simple change of variables to polar coordinates starting from (B2) and is left to the reader. The two limiting cases in which the variable $r$ approaches zero or infinity confirm that the proposed normalized areal measure is bounded in the interval between zero and unity.

Finally, the normalized circumference of the simple closed curve, as depicted in Fig. 2(A), is given by

$$\Lambda(a,b) = \frac{2}{\pi b\sqrt{1+a^2}}\left((1+b^2)\,\Pi\left(\frac{a^2-b^2}{1+a^2}, \omega\right) - \mathrm{K}(\omega)\right) \quad (34)$$

where $\omega \equiv (b^2-a^2)/((1+a^2)b^2)$.

Again, the normalized circumferential measure is also a dimensionless quantity. The derivation of (34) is provided in Appendices V and VI. When $r \equiv a = b$, the normalized circumferential measure is reduced to

$$\Lambda = \frac{r}{\sqrt{1+r^2}}.$$

It is only when $a = b$ that $\Gamma$ is in one to one correspondence to $\Lambda$, i.e., $\Gamma = 1-(\Lambda/r)$. In general, $\Gamma$ maps to multiple $\Lambda$ and vice versa.

## III. Results

We shall outline the basic idea of constructing the covariance matrix of the major eigenvector of the diffusion tensor with an example similar to that presented in [25] and [47]. The technique of error propagation via diffusion tensor representations will be denoted by "EP" while the reformulated perturbation technique described in the previous section will be denoted by "RP." We will take a synthetic diffusion tensor, given by

$$\boldsymbol{\gamma} = [\ln(1000)\times 10^{+4}\,\mathrm{s/mm^2}, 9.475, 6.694, 4.829, 1.123, -0.507, -1.63]^T \times 10^{-4}\mathrm{mm^2/s}$$

as known. The eigenvalue-eigenvector pairs of this tensor are

$$\{10.4\times 10^{-4}\ \mathrm{mm^2/s}, \mathbf{q_1} = [0.9027, 0.3139, -0.2940]^T\}$$
$$\{6.30\times 10^{-4}\ \mathrm{mm^2/s}, \mathbf{q}_2 = [0.3197, -0.9470, -0.0295]^T\}$$

and

$$\{4.30\times 10^{-4}\ \mathrm{mm^2/s}, \mathbf{q}_3 = [0.2877, 0.0673, 0.9553]^T\}.$$

Further, the trace and the fractional anisotropy (FA) of this synthetic diffusion tensor are 0.0021 mm$^2$/s and 0.4176, respectively.

The mean covariance matrix of the major eigenvector of this tensor, based on EP and RP is essentially equivalent except for some rounding errors

$${}_{\mathrm{RP}}\boldsymbol{\Sigma}_{\mathbf{q}_1} \approx {}_{\mathrm{EP}}\boldsymbol{\Sigma}_{\mathbf{q}_1} = \begin{pmatrix} 6.0911 & -13.269 & 4.5350 \\ -13.269 & 40.379 & 2.3675 \\ 4.5350 & 2.3675 & 16.450 \end{pmatrix} \times 10^{-5}.$$

Full details on this and related computations that require the notion of average covariance can be found in [25] and [47].

The computation above is carried out based on a signal-to-noise ratio (SNR) of 50 and on a design matrix $\mathbf{W}$ that was constructed from a 35 gradient direction set with four spherical shells having $b$ values of 0, 500, 1000, and 1500 s/mm$^2$.

The eigenvalue-eigenvector pairs of ${}_{\mathrm{EP}}\boldsymbol{\Sigma}_{\mathbf{q}_1}$ are

$$\{\omega_1 = 4.4935\times 10^{-4}, [0.3202, -0.9469, -0.0277]^T\}$$
$$\{\omega_2 = 1.7985\times 10^{-4}, [0.2871, 0.0691, 0.9553]^T\}$$

and

$$\{\omega_3 = 4.387\times 10^{-20} \cong 0, [0.9027, 0.3139, -0.2940]^T\}.$$

Finally, the only difference between the eigenvalue-eigenvector pairs of ${}_{\mathrm{EP}}\boldsymbol{\Sigma}_{\mathbf{q}_1}$ and of ${}_{\mathrm{RP}}\boldsymbol{\Sigma}_{\mathbf{q}_1}$ is in the minor eigenvalue,

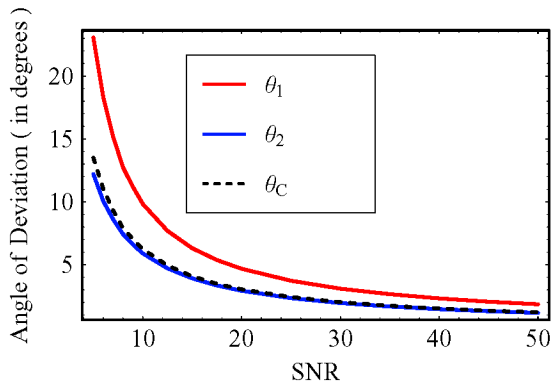


Fig. 3. The angle of deviation (in degrees) as a function of SNR.The red curve, $\theta_1$, and the blue curve, $\theta_2$, denote the angles of deviation of the major and the minor axes of the elliptical cone of uncertainty, respectively. The dotted curve, $\theta_C$, denotes the angle of deviation of the circular cone. At each SNR, 5000 samples were generated to obtain an estimated angle of deviation.

$2.5243 \times 10^{-20}$ for ${}_{\mathrm{RP}}\mathbf{\Sigma}_{\mathbf{q}_1}$, which is of no consequence in practice.

Although it is interesting to compare the angle of deviation of the two major axes of the elliptical COU to that of the circular COU, a consistent comparison cannot be easily made because the formalism used in the circular COU, (26), is ill-suited for establishing the joint confidence region for the major eigenvector. Specifically, the angle of deviation of the circular COU is derived from a hyper-cuboid region in the space of the diffusion tensor elements determined by $\delta\mathbf{D}$ rather than from a confidence region in the space of the elements of the major eigenvector. With this issue in mind, we will present a qualitative comparison by adjusting the confidence level $1-\alpha$ of the elliptical COU. Here, we will take $\alpha$ to be 0.3173, which is the area covering the two tails of the normal distribution at one standard deviation apart from the center, i.e., at $-1$ and $+1$. Therefore, we have $\mathcal{F}(2, 140-7; 0.3173) = 1.1578$ for this particular example.

The angle of deviation for the principal directions of the elliptical COU are given by $\theta_1 = \tan^{-1}(\sqrt{2\mathcal{F}(2, n-7; \alpha)\omega_1})$, and $\theta_2 = \tan^{-1}(\sqrt{2\mathcal{F}(2, n-7; \alpha)\omega_2})$, respectively, where $\omega_1$ and $\omega_2$ are the first two largest eigenvalues of ${}_{\mathrm{RP}}\mathbf{\Sigma}_{\mathbf{q}_1}$. In the context of the example discussed here, we have $\theta_1 = 1.847°$ and $\theta_2 = 1.169°$ while the angle of deviation of the circular cone of uncertainty is $\theta_C = 1.211°$. We also show here the SNR dependence of $\theta_1, \theta_2$, and $\theta_C$ based on the same design matrix and the underlying true tensor, see Fig. 3.

Using the same simulated human brain tensor data used in [37] and [25], [47] together with the experimental design defined in the above example, the normalized areal measure map, which corresponds to the 0.95 joint confidence region (or 95% confidence region) at an SNR level of 15, can be obtained and is shown in Fig. 4(C) while the corresponding image of the cones of uncertainty is shown in Fig. 5. Fig. 4(A) and (B) show the FA map and the cones of uncertainty within the region bounded by the rectangular box indicated in Fig. 4(A). Fig. 4(D) and (E) are, respectively, the normalized circumference map, see Appendix V, and the eccentricity map of the ellipse of the cone of uncertainty. The eccentricity of an ellipse is given by $(1 - b^2/a^2)^{1/2}$ and it is assumed that $b \leq a$.

## IV. Discussion

In this work, one of our main objectives is to elucidate the connection between the first-order matrix perturbation method and the error propagation method via diffusion tensor representations by way of an important example—the covariance of the major eigenvector of the diffusion tensor, and to show that these two methods are distinct but complementary. The other main objective is to provide new normalized scalar measures related to the cone of uncertainty and to outline a new technique of visualizing the cone of uncertainty.

The covariance matrices of the eigenvector of the diffusion tensor as obtained from the perturbation method and the error propagation method via diffusion tensor representations are *in principle* equivalent, but are *in practice* very different; the first-order matrix perturbation as reformulated here is simpler, and therefore, more efficient than the approach via diffusion tensor representations. However, the error propagation via Euler representation is more coherent in that the uncertainty of any tensor-derived quantity, scalar-valued or vector-valued, can be obtained from the Euler representation alone while the first-order matrix perturbation method requires two distinctly different representations. Consequently, two Jacobian matrices of the eigenvalues and of the eigenvectors with respect to the ordinary tensor representation are needed in the first-order matrix perturbation method. It is important to note that the reformulation of the first-order matrix perturbation method proposed in this work makes the perturbation method practical for 3-D visualization of the cones of uncertainty. We should also point out that the proposed reformulation makes use of the covariance matrix of the diffusion tensor that is derived from the nonlinear objective function of diffusion tensor estimation [25], [47], [37].

Here, we outline the main findings of this work. First, the perturbation method is reformulated to obtain the covariance of the major eigenvector of the diffusion tensor. Second, this covariance matrix is shown to be equivalent to that derived from the error propagation method based on the Euler representation. Third, when a mapping between representations of interest is not available then it is likely that the first-order matrix perturbation method may be helpful in finding the Jacobian matrix so that the transformation from one covariance structure to another can be realized. Finally, two new normalized measures of the cone of uncertainty and a new technique of visualizing the cone of uncertainty are described.

In DT-MRI studies, several scalar measures have been proposed to characterize tract dispersion; some are parametric [17], [20], [25], [47], [29] while others are not [18], [19], [28]. The normalized circumferential and areal measures discussed in this work belong to the former and can be viewed as a local parametric coherence measure. Since the major eigenvector of the diffusion tensor is usually associated with the directional preference of the diffusing water molecules, the proposed measures, which are directly linked to the uncertainty in the major eigenvector of the diffusion tensor, may be important for probing the integrity of the white matter tracts in the brain. In addition to that, these measures have a dependence on the signal-to-noise

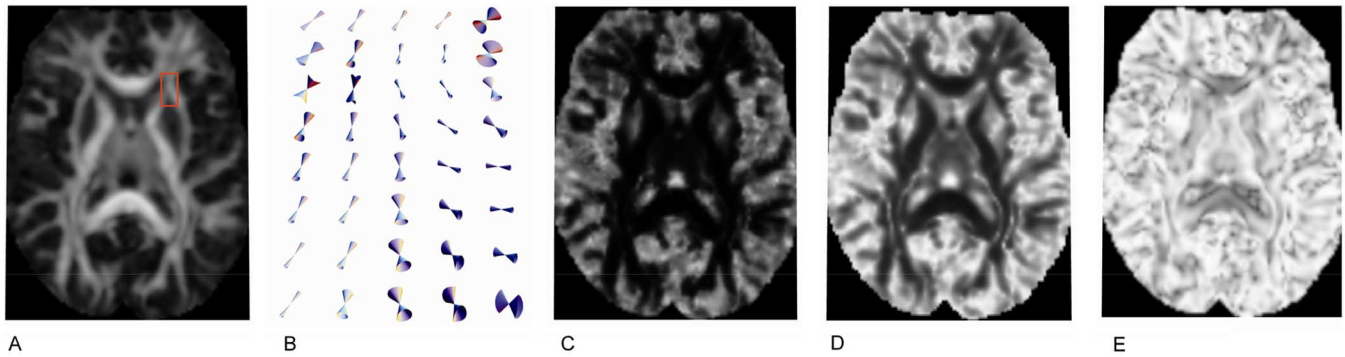


Fig. 4. (A) A fractional anisotropy (FA) map. (B) The corresponding elliptical 95% confidence cones of uncertainty on the region bounded by the red rectangular box in (A) at an SNR level of 15. (C) The map of the normalized areal measure and (D) the map of the normalized circumferential measure. (E) The map of the eccentricity of the ellipse of the 95% confidence COU. The maps, (C), (D), and (E), are generated from the 95% confidence COU at ant SNR level of 15. Let the minimum value, the lower quartile, the median, the upper quartile and the maximum value of a map (excluding the background) be arranged as an array of five elements in ascending order. The arrays associated with (A), (C), (D), and (E) are approximately and respectively {0.013, 0.078, 0.145, 0.299, 0.873}, {0.001, 0.021, 0.091, 0.239, 0.828}, {0.047, 0.216, 0.455, 0.700, 0.997}, and {0.102, 0.688, 0.817, 0.908, 0.999}.

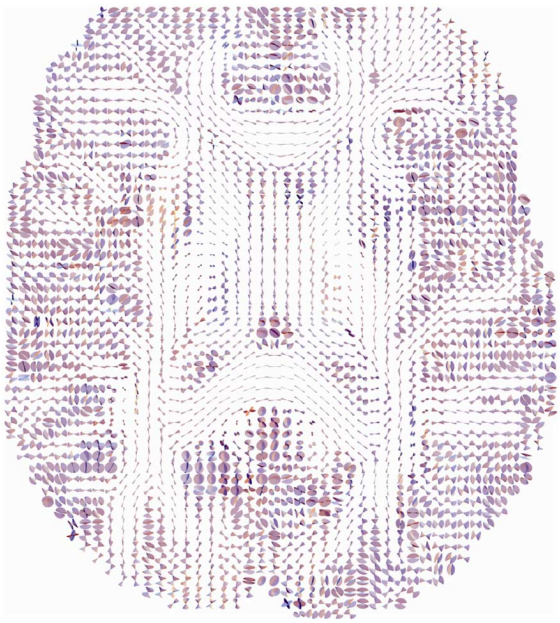

Fig. 5. An axial slice of the map of 95% confidence COU at an SNR level of 15.

ratio and may be used as a calibration gauge for assessing an MRI system or DT-MRI acquisition performance.

The key advantage of the proposed measures for quantifying uncertainty of the major eigenvector of the diffusion tensor is that these measures are dimensionless and normalized to unity. These measures have direct geometric interpretations. In particular, the areal measure corresponds directly to the projection of the $1-\alpha$ joint confidence region for $\mathbf{q}_1$ in the $u, v$-plane onto the unit sphere. Besides the areal measure, the circumferential measure may be important in gaining insights into the asymmetric nature of tract dispersion. It should be clear that the dispersion information contained in $\mathbf{\Sigma}_{\mathbf{q}_1}$ may be incorporated into modeling the prior distribution of fiber coherence in probabilistic (or Bayesian) tractography [23], [24], [32]. Finally, we should note that the main motivation behind the proposed technique of COU construction is to avoid overlapping cones of uncertainty from neighboring regions.

Readers of Hext's work [33] will soon realize that hidden in the seemingly innocent phrase "*in vector notation*," which appeared on the line just above (4.21) in [33], lies the main hurdle in rendering that formulation suitable for practical computation and visualization. We hope the present study and our earlier work [25], [47] prepare readers to look at Hext's work from an illuminating vantage point where the fundamental connection between the first-order matrix perturbation method and the error propagation method is elucidated and the role of the Jacobian matrix is highlighted.

## V. Conclusion

Building upon the covariance matrix of the diffusion tensor that is derived from the nonlinear least squares method, the first-order matrix perturbation is reformulated and shown to be equivalent to the technique of error propagation via diffusion tensor representations in expressing the covariance of the major eigenvector of the diffusion tensor. Normalized circumferential and areal measures of the uncertainty of the major eigenvector and a new technique of constructing the cone of uncertainty are explicated.

## Appendix A
## Notations

Here, we describe the notations used in this work. The diffusion tensor $\mathbf{D}$ is a $3 \times 3$ symmetric positive definite matrix given by

$$\begin{pmatrix} D_{xx} & D_{xy} & D_{xz} \\ D_{xy} & D_{yy} & D_{yz} \\ D_{xz} & D_{yz} & D_{zz} \end{pmatrix}.$$

The measured (noisy) DW signals are denoted by $s_i$, while the DW functions at $\boldsymbol{\gamma}$ or $\boldsymbol{\gamma}(\boldsymbol{\xi})$ are $\hat{s}_i(\boldsymbol{\gamma}) = \exp[\sum_{j=1}^{7} W_{ij}\gamma_j]$ and

$\hat{s}_i(\boldsymbol{\gamma}(\boldsymbol{\xi})) = \exp[\sum_{j=1}^{7} W_{ij}\gamma_j(\boldsymbol{\xi})]$, respectively. Supposing that $\hat{\boldsymbol{\gamma}}_{\mathrm{NLS}}$ is the nonlinear least squares estimate of the parameter vector $\boldsymbol{\gamma}$, then the residual vector is a vector whose individual component is the difference between the observed and the expected or estimated signals

$$\mathbf{r}(\hat{\boldsymbol{\gamma}}_{\mathrm{NLS}}) = [r_1(\hat{\boldsymbol{\gamma}}_{\mathrm{NLS}}) \quad \cdots \quad r_n(\hat{\boldsymbol{\gamma}}_{\mathrm{NLS}})]^T$$

where $r_i(\hat{\boldsymbol{\gamma}}_{\mathrm{NLS}}) = s_i - \hat{s}_i(\hat{\boldsymbol{\gamma}}_{\mathrm{NLS}})$ for $i = 1, \ldots, n$.

The design matrix $\mathbf{W}$ is given by at the bottom of the page.

The two representations of the diffusion tensor, which will be used in this work, are the ordinary diffusion tensor representation, given by

$$\begin{aligned}\boldsymbol{\gamma} &= [\gamma_1, \gamma_2, \gamma_3, \gamma_4, \gamma_5, \gamma_6, \gamma_7]^T \\ &= [\ln(s_0), D_{xx}, D_{yy}, D_{zz}, D_{xy}, D_{yz}, D_{xz}]^T\end{aligned}$$

and the Euler diffusion tensor representation given by

$$\begin{aligned}\boldsymbol{\xi} &= [\xi_1, \xi_2, \xi_3, \xi_4, \xi_5, \xi_6, \xi_7]^T \\ &= [\ln(s_0), \lambda_1, \lambda_2, \lambda_3, \theta, \phi, \psi]^T\end{aligned}$$

where $s_0$ is the parameter for the nondiffusion weighted signal. The major, medium, and minor eigenvalues are denoted by $\lambda_1, \lambda_2$, and $\lambda_3$, respectively. The Euler angles are denoted by $\theta, \phi$, and $\psi$, respectively. Since there are many conventions that can be used to parametrize the rotation matrix using the Euler angles, we will adopt the convention that is consistent with our previous work [25], [47].

The matrices $\mathbf{S}$ and $\hat{\mathbf{S}}$ are diagonal matrices whose diagonal elements are the observed and the estimated diffusion weighted signals, respectively, i.e.,

$$\mathbf{S} = \begin{pmatrix} s_1 & & \\ & \ddots & \\ & & s_n \end{pmatrix} \quad \text{and} \quad \hat{\mathbf{S}} = \begin{pmatrix} \hat{s}_1 & & \\ & \ddots & \\ & & \hat{s}_n \end{pmatrix}.$$

The residual matrix is expressed as: $\mathbf{R} = \mathbf{S} - \hat{\mathbf{S}}$. The element of the Jacobian matrix, $\mathbf{J}_{\boldsymbol{\rho}}(\boldsymbol{\gamma})$, is defined as $[\mathbf{J}_{\boldsymbol{\rho}}(\boldsymbol{\gamma})]_{ij} \equiv \partial\gamma_i/\partial\rho_j$. Similarly, we have $[\mathbf{J}_{\boldsymbol{\xi}}(\boldsymbol{\gamma})]_{ij} \equiv \partial\gamma_i/\partial\xi_j$. Finally, $\sigma^2_{DW}$ is the estimated variance derived from the nonlinear fit (1), i.e., $\sigma^2_{DW} = 2f_{\mathrm{NLS}}(\hat{\boldsymbol{\gamma}}_{\mathrm{NLS}})/(n-7)$, see also [25], [47], and [37].

## Appendix B

In this Appendix, we will derive (32). First, we evaluate several preliminary expressions

$$\begin{aligned}\frac{\partial X_s}{\partial u} &= \frac{1+v^2}{(u^2+v^2+1)^{3/2}}, \\ \frac{\partial X_s}{\partial v} &= -\frac{uv}{(u^2+v^2+1)^{3/2}} = \frac{\partial Y_s}{\partial u} \\ \frac{\partial Y_s}{\partial v} &= \frac{1+u^2}{(u^2+v^2+1)^{3/2}} \\ \frac{\partial Z_s}{\partial u} &= -\frac{u}{(u^2+v^2+1)^{3/2}}, \\ \frac{\partial Z_s}{\partial v} &= -\frac{v}{(u^2+v^2+1)^{3/2}} \\ E &= \left(\frac{\partial X_s}{\partial u}\right)^2 + \left(\frac{\partial Y_s}{\partial u}\right)^2 + \left(\frac{\partial Z_s}{\partial u}\right)^2 \\ &= \frac{1+v^2}{(u^2+v^2+1)^2} \\ G &= \left(\frac{\partial X_s}{\partial v}\right)^2 + \left(\frac{\partial Y_s}{\partial v}\right)^2 + \left(\frac{\partial Z_s}{\partial v}\right)^2 \\ &= \frac{1+u^2}{(u^2+v^2+1)^2}\end{aligned}$$

and

$$\begin{aligned}F &= \frac{\partial X_s}{\partial u}\frac{\partial X_s}{\partial v} + \frac{\partial Y_s}{\partial u}\frac{\partial Y_s}{\partial v} + \frac{\partial Z_s}{\partial u}\frac{\partial Z_s}{\partial v} \\ &= -\frac{uv}{(u^2+v^2+1)^2}.\end{aligned}$$

The integrand in (31) is then given by

$$\begin{aligned}\sqrt{EG-F^2} &= \sqrt{\frac{(1+v^2)(1+u^2)}{(u^2+v^2+1)^4} - \frac{u^2v^2}{(u^2+v^2+1)^4}} \\ &= \frac{1}{(u^2+v^2+1)^{3/2}}.\end{aligned}$$

Therefore

$$\Gamma = \frac{1}{2\pi}\iint_R \frac{1}{(u^2+v^2+1)^{3/2}}\,du\,dv, \tag{B1}$$

where $R$ is the region defined by $(u/a)^2 + (v/b)^2 \le 1$.

By a change of variables, $u = a\xi_x$ and $v = b\xi_y$, we obtain

$$\Gamma = \frac{ab}{2\pi}\iint_{R_1} \frac{1}{(1+a^2\xi_x^2+b^2\xi_y^2)^{3/2}} d\xi_x\,d\xi_y \tag{B2}$$

where $R_1$ is a circular region (or a disk) defined by $\xi_x^2 + \xi_y^2 \le 1$. The limits of integration due to $R_1$ can be introduced into $\Gamma$ and the integral is now given by

$$\Gamma = \frac{ab}{2\pi}\int_{-1}^{1}\int_{-\sqrt{1-\xi_y^2}}^{\sqrt{1-\xi_y^2}} \frac{1}{(1+a^2\xi_x^2+b^2\xi_y^2)^{3/2}} d\xi_x\,d\xi_y. \tag{B3}$$

$$\begin{pmatrix} 1 & -b_1g_{1x}^2 & -b_1g_{1y}^2 & -b_1g_{1z}^2 & -2b_1g_{1x}g_{1y} & -2b_1g_{1y}g_{1z} & -2b_1g_{1x}g_{1z} \\ \vdots & \vdots & \vdots & \vdots & \vdots & \vdots & \vdots \\ 1 & -b_ng_{nx}^2 & -b_ng_{ny}^2 & -b_ng_{nz}^2 & -2b_ng_{nx}g_{ny} & -2b_ng_{ny}g_{nz} & -2b_ng_{nx}g_{nz} \end{pmatrix}$$

Factoring out the term $a^2$ in the integrand and defining $\beta^2 \equiv (1+b^2\xi_y^2)/a^2$, the inner integral can be evaluated using the result in Appendix III-(C1), so that we have

$$\begin{aligned}\Gamma &= \frac{b}{2\pi a^2}\int_{-1}^{1}\left[\frac{1}{\beta^2}\xi_x(\beta^2+\xi_x^2)^{-\frac{1}{2}}\right]_{\xi_x=-\sqrt{1-\xi_y^2}}^{\xi_x=+\sqrt{1-\xi_y^2}} d\xi_y \\ &= \frac{b}{\pi a^2}\int_{-1}^{1}\left[\frac{1}{\beta^2}\sqrt{1-\xi_y^2}\left(\beta^2+1-\xi_y^2\right)^{-\frac{1}{2}}\right] d\xi_y \\ &= \frac{ab}{\pi}\int_{-1}^{1}\left[\frac{\sqrt{1-\xi_y^2}}{1+b^2\xi_y^2}\frac{1}{\left(1+b^2\xi_y^2+a^2-a^2\xi_y^2\right)^{1/2}}\right] d\xi_y.\end{aligned}$$

Because the integrand is an even function, we can write

$$\begin{aligned}\Gamma &= \frac{2ab}{\pi}\int_{0}^{1}\left[\frac{\sqrt{1-\xi_y^2}}{1+b^2\xi_y^2}\frac{1}{\left(1+b^2\xi_y^2+a^2-a^2\xi_y^2\right)^{1/2}}\right] d\xi_y \\ &= \frac{2ab}{\pi\sqrt{1+a^2}} \\ &\quad\times\int_{0}^{1}\left[\frac{1-\xi_y^2}{1+b^2\xi_y^2}\frac{1}{(1-\xi_y^2)^{1/2}(1-\frac{a^2-b^2}{1+a^2}\xi_y^2)^{1/2}}\right] d\xi_y.\end{aligned}$$

By the result of Appendix IV, we have

$$\begin{aligned}\Gamma &= \frac{2ab}{\pi\sqrt{1+a^2}} \\ &\quad\times\left(\left(1+\frac{1}{b^2}\right)\Pi\left(-b^2,\frac{a^2-b^2}{1+a^2}\right)-\frac{1}{b^2}\mathrm{K}\left(\frac{a^2-b^2}{1+a^2}\right)\right) \\ &= \frac{2a}{\pi b\sqrt{1+a^2}} \\ &\quad\times\left((1+b^2)\Pi\left(-b^2,\frac{a^2-b^2}{1+a^2}\right)-\mathrm{K}\left(\frac{a^2-b^2}{1+a^2}\right)\right).\end{aligned} \tag{B4}$$

It is interesting to note that a new mathematical identity shows itself quite readily since $\Gamma$ should be invariant with respect to the permutation of $a$ and $b$.

## Appendix C

We will derive an expression for this integral which is needed in Appendix II

$$\int\frac{1}{(\beta^2+\xi^2)^{3/2}}d\xi.$$

Define $\mathrm{T} = \xi(\beta^2+\xi^2)^{-(m/2)+1}$, the derivative of T with respect to $\xi$ is given by

$$\begin{aligned}d\mathrm{T}/d\xi &= (\beta^2+\xi^2)^{-\frac{m}{2}+1}-\xi^2(m-2)(\beta^2+\xi^2)^{-\frac{m}{2}} \\ &= (\beta^2+\xi^2)^{-\frac{m}{2}+1} \\ &\quad-((\beta^2+\xi^2)-\beta^2)(m-2)(\beta^2+\xi^2)^{-\frac{m}{2}} \\ &= (\beta^2+\xi^2)^{-\frac{m}{2}+1}-(m-2)(\beta^2+\xi^2)^{-\frac{m}{2}+1} \\ &\quad+\beta^2(m-2)(\beta^2+\xi^2)^{-\frac{m}{2}} \\ &= (3-m)(\beta^2+\xi^2)^{-\frac{m}{2}+1} \\ &\quad+\beta^2(m-2)(\beta^2+\xi^2)^{-\frac{m}{2}}.\end{aligned}$$

Rearranging $\beta^2(m-2)$ in the equation above, we have

$$(\beta^2+\xi^2)^{-\frac{m}{2}} = \frac{(3-m)}{\beta^2(m-2)}(\beta^2+\xi^2)^{-\frac{m}{2}+1}+\frac{1}{\beta^2(m-2)}\frac{d\mathrm{T}}{d\xi}.$$

Therefore

$$\begin{aligned}\int(\beta^2+\xi^2)^{-\frac{m}{2}}d\xi &= \frac{(3-m)}{\beta^2(m-2)} \\ &\quad\times\int(\beta^2+\xi^2)^{-\frac{m}{2}+1}d\xi+\frac{1}{\beta^2(m-2)}\xi(\beta^2+\xi^2)^{-\frac{m}{2}+1}.\end{aligned}$$

It is clear that

$$\int(\beta^2+\xi^2)^{-\frac{3}{2}}d\xi = \frac{1}{\beta^2}\xi(\beta^2+\xi^2)^{-\frac{1}{2}}. \tag{C1}$$

A faster, more direct but less general approach (not shown here) would be to make a trigonometric substitution of $\tan\theta = \xi/\beta$.

## Appendix D

The goal of this Appendix is to express the integral below in terms of the complete elliptic integrals of the first and third kinds:

$$I = \int_{0}^{1}\left[\frac{1-\xi_y^2}{1+b^2\xi_y^2}\frac{1}{(1-\xi_y^2)^{1/2}\left(1-\frac{a^2-b^2}{1+a^2}\xi_y^2\right)^{1/2}}\right] d\xi_y. \tag{D1}$$

Define

$$d_1 = \frac{1}{1+b^2\xi_y^2}\frac{1}{(1-\xi_y^2)^{1/2}\left(1-\frac{a^2-b^2}{1+a^2}\xi_y^2\right)^{1/2}}$$

and

$$d_2 = \frac{1}{\left(1-\xi_y^2\right)^{1/2}\left(1-\frac{a^2-b^2}{1+a^2}\xi_y^2\right)^{1/2}}$$

we then have

$$\mathrm{K}\left(\frac{a^2-b^2}{1+a^2}\right) = \int_{0}^{1}\frac{1}{d_2}d\xi_y$$

and

$$\Pi\left(-b^2,\frac{a^2-b^2}{1+a^2}\right) = \int_{0}^{1}\frac{1}{d_1}d\xi_y.$$

It is easy to see that

$$I = \int_{0}^{1}\left[\frac{1-\xi_y^2}{1+b^2\xi_y^2}\frac{1}{d_2}\right] d\xi_y$$

and

$$I = \int_{0}^{1}\left[\frac{1-\xi_y^2}{d_1}\right] d\xi_y$$

are both valid. The former leads to

$$\begin{aligned} I &= \int_0^1 \left[\frac{1-\xi_y^2+b^2\xi_y^2-b^2\xi_y^2}{1+b^2\xi_y^2}\frac{1}{d_2}\right]d\xi_y \\ &= \int_0^1 \left[\frac{1+b^2\xi_y^2-(1+b^2)\xi_y^2}{1+b^2\xi_y^2}\frac{1}{d_2}\right]d\xi_y \\ &= \int_0^1 \frac{1}{d_2}d\xi_y - (1+b^2)\int_0^1 \frac{\xi_y^2}{d_1}d\xi_y \\ &= \mathrm{K}\left(\frac{a^2-b^2}{1+a^2}\right) - (1+b^2)\int_0^1 \frac{\xi_y^2}{d_1}d\xi_y \end{aligned} \tag{D2}$$

while the latter leads to

$$\begin{aligned} I &= \int_0^1 \left[\frac{1-\xi_y^2}{d_1}\right]d\xi_y \\ &= \int_0^1 \frac{1}{d_1}d\xi_y - \int_0^1 \frac{\xi_y^2}{d_1}\,d\xi_y \\ &= \Pi\left(-b^2, \frac{a^2-b^2}{1+a^2}\right) - \int_0^1 \frac{\xi_y^2}{d_1}d\xi_y. \end{aligned} \tag{D3}$$

Since (D1) and (D2) are equivalent, we can equate them

$$\begin{aligned} &\mathrm{K}\left(\frac{a^2-b^2}{1+a^2}\right) - (1+b^2)\int_0^1 \frac{\xi_y^2}{d_1}d\xi_y \\ &\quad = \Pi\left(-b^2, \frac{a^2-b^2}{1+a^2}\right) - \int_0^1 \frac{\xi_y^2}{d_1}d\xi_y \end{aligned}$$

so that

$$\int_0^1 \frac{\xi_y^2}{d_1}d\xi_y = -\frac{1}{b^2}\left(\Pi\left(-b^2, \frac{a^2-b^2}{1+a^2}\right)\mathrm{K}\left(\frac{a^2-b^2}{1+a^2}\right)\right). \tag{D4}$$

The integral, $I$, can now be expressed in terms of K and $\Pi$

$$\begin{aligned} I &= \Pi\left(-b^2, \frac{a^2-b^2}{1+a^2}\right) - \int_0^1 \frac{\xi_y^2}{d_1}, d\xi_y \\ &= \Pi\left(-b^2, \frac{a^2-b^2}{1+a^2}\right) \\ &\quad + \frac{1}{b^2}\left(\Pi\left(-b^2, \frac{a^2-b^2}{1+a^2}\right) - \mathrm{K}\left(\frac{a^2-b^2}{1+a^2}\right)\right) \\ &= \left(1+\frac{1}{b^2}\right)\Pi\left(-b^2, \frac{a^2-b^2}{1+a^2}\right) \\ &\quad - \frac{1}{b^2}\mathrm{K}\left(\frac{a^2-b^2}{1+a^2}\right). \end{aligned} \tag{D5}$$

## APPENDIX E

In this Appendix, the circumference of a simple closed curve on the sphere shown in Fig. 2(A) is expressed in terms of the complete elliptical integrals of the first and third kinds. The normalized circumference of the simple closed curve on the unit sphere can be defined as

$$\Lambda = \frac{1}{2\pi}\int_0^{2\pi}\sqrt{\left(\frac{dX_s(\theta)}{d\theta}\right)^2 + \left(\frac{dY_s(\theta)}{d\theta}\right)^2 + \left(\frac{dZ_s(\theta)}{d\theta}\right)^2}d\theta. \tag{E1}$$

The $2\pi$ in the denominator is the normalization factor coming from the circumference of the great circle of the unit sphere. Without loss of generality, we parametrize the components of the vector, $\mathbf{s}$, in terms of $a, b$, and $\theta$ as follows:

$$\begin{aligned} \mathbf{s}(\theta) &\equiv \begin{pmatrix} X_s(\theta) \\ Y_s(\theta) \\ Z_s(\theta) \end{pmatrix} \\ &= \begin{pmatrix} \frac{a\cos(\theta)}{\sqrt{(a\cos(\theta))^2+(b\sin(\theta))^2+1}} \\ \frac{b\sin(\theta)}{\sqrt{(a\cos(\theta))^2+(b\sin(\theta))^2+1}} \\ \frac{1}{\sqrt{(a\cos(\theta))^2+(b\sin(\theta))^2+1}} \end{pmatrix}. \end{aligned}$$

Equation (E1) can be further simplified and expressed in terms of the complete elliptic integrals of the first and third kinds:

$$\begin{aligned} \Lambda(a,b) &= \frac{2}{\pi b\sqrt{1+a^2}} \\ &\quad \times \left((1+b^2)\Pi\left(\frac{a^2-b^2}{1+a^2}, \omega\right) - \mathrm{K}(\omega)\right) \end{aligned} \tag{E2}$$

where $\omega = (b^2-a^2)/((1+a^2)b^2)$.

The derivation of (E2) is provided in Appendix VI.

## APPENDIX F

In this Appendix, our goal is to derive (E2) starting from (E1). Provided here are several preliminary expressions

$$\begin{aligned} &(dX_s(\theta)/d\theta)^2 \\ &\quad = \frac{a^2(1+b^2)^2\sin^2(\theta)}{[1+a^2-(a^2-b^2)\sin^2(\theta)]^3} \\ &(dY_s(\theta)/d\theta)^2 \\ &\quad = \frac{b^2(1+a^2)^2\cos^2(\theta)}{[1+a^2-(a^2-b^2)\sin^2(\theta)]^3} \\ &(dZ_s(\theta)/d\theta)^2 \\ &\quad = \frac{(b^2-a^2)^2\sin^2(\theta)\cos^2(\theta)}{[1+a^2-(a^2-b^2)\sin^2(\theta)]^3} \\ &\Phi \equiv (dX_s(\theta)/d\theta)^2 + (dY_s(\theta)/d\theta)^2 \\ &\qquad + (dZ_s(\theta)/d\theta)^2, \\ &\quad = \frac{a^2(1+b^2)^2\sin^2(\theta) + b^2(1+a^2)^2\cos^2(\theta)}{[1+a^2-(a^2-b^2)\sin^2(\theta)]^3} \\ &\qquad + \frac{(b^2-a^2)^2\sin^2(\theta)\cos^2(\theta)}{[1+a^2-(a^2-b^2)\sin^2(\theta)]^3}. \end{aligned}$$

With some algebraic manipulations, it can be shown that

$$\Phi = \frac{(b^2(1+a^2)+(a^2-b^2)\sin^2(\theta))}{[1+a^2-(a^2-b^2)\sin^2(\theta)]^3} \times(1+a^2-(a^2-b^2)\sin^2(\theta))$$

so that the square root of $\Phi$ may be written as

$$\sqrt{\Phi} = \frac{\sqrt{b^2(1+a^2)+(a^2-b^2)\sin^2(\theta)}}{[1+a^2-(a^2-b^2)\sin^2(\theta)]}$$

or

$$\begin{aligned}\sqrt{\Phi} &= \frac{b^2(1+a^2)+(a^2-b^2)\sin^2(\theta)}{[1+a^2-(a^2-b^2)\sin^2(\theta)]} \\ &\quad\times \frac{1}{\sqrt{b^2(1+a^2)+(a^2-b^2)\sin^2(\theta)}} \\ &= \frac{b}{(1+a^2)^{1/2}} \\ &\quad\times \frac{1-\frac{(b^2-a^2)}{b^2(1+a^2)}\sin^2(\theta)}{\left[1-\frac{(a^2-b^2)}{(1+a^2)}\sin^2(\theta)\right]\sqrt{1-\frac{(b^2-a^2)}{b^2(1+a^2)}\sin^2(\theta)}}.\end{aligned}$$

The normalized circumference is then given by

$$\Lambda = \frac{1}{2\pi}\int_0^{2\pi}\sqrt{\Phi}d\theta.$$

Since the arc length for each quadrant is the same, the normalized circumference, $\Lambda$, can be reduced to

$$\begin{aligned}\Lambda &= \frac{2}{\pi}\int_0^{\pi/2}\sqrt{\Phi}d\theta \\ \Lambda &= \frac{2b}{\pi(1+a^2)^{1/2}} \\ &\quad\times\int_0^{\pi/2}\frac{1-\frac{(b^2-a^2)}{b^2(1+a^2)}\sin^2(\theta)}{\left[1-\frac{(a^2-b^2)}{(1+a^2)}\sin^2(\theta)\right]\sqrt{1-\frac{(b^2-a^2)}{b^2(1+a^2)}\sin^2(\theta)}}d\theta.\end{aligned} \tag{F1}$$

Similar to the technique used in Appendix IV, let us express the integral in (F1) in two different but equivalent ways, as shown in the equation at the bottom of the page.

Since the two expressions $I_1$ and $I_2$ are equivalent, we can solve for $II$ by equating the two expressions so that $II$ is given

$$\begin{aligned}I_1 &= \int_0^{\pi/2}\frac{1-\frac{(a^2-b^2)}{(1+a^2)}\sin^2(\theta)+\frac{(a^2-b^2)}{(1+a^2)}\sin^2(\theta)-\frac{(b^2-a^2)}{b^2(1+a^2)}\sin^2(\theta)}{\left[1-\frac{(a^2-b^2)}{(1+a^2)}\sin^2(\theta)\right]\sqrt{1-\frac{(b^2-a^2)}{b^2(1+a^2)}\sin^2(\theta)}}d\theta \\ &= \int_0^{\pi/2}\frac{1}{\sqrt{1-\frac{(b^2-a^2)}{b^2(1+a^2)}\sin^2(\theta)}}d\theta+\left(\frac{(a^2-b^2)}{(1+a^2)}-\frac{(b^2-a^2)}{b^2(1+a^2)}\right) \\ &\quad\times\underbrace{\int_0^{\pi/2}\frac{\sin^2(\theta)}{\left[1-\frac{(a^2-b^2)}{(1+a^2)}\sin^2(\theta)\right]\sqrt{1-\frac{(b^2-a^2)}{b^2(1+a^2)}\sin^2(\theta)}}d\theta}_{II} \\ &= \mathrm{K}\left(\frac{(b^2-a^2)}{b^2(1+a^2)}\right)+\left(\frac{(a^2-b^2)}{(1+a^2)}-\frac{(b^2-a^2)}{b^2(1+a^2)}\right)II \\ I_2 &= \int_0^{\pi/2}\frac{1-\frac{(b^2-a^2)}{b^2(1+a^2)}\sin^2(\theta)}{\left[1-\frac{(a^2-b^2)}{(1+a^2)}\sin^2(\theta)\right]\sqrt{1-\frac{(b^2-a^2)}{b^2(1+a^2)}\sin^2(\theta)}}d\theta \\ &= \int_0^{\pi/2}\frac{1}{\left[1-\frac{(a^2-b^2)}{(1+a^2)}\sin^2(\theta)\right]\sqrt{1-\frac{(b^2-a^2)}{b^2(1+a^2)}\sin^2(\theta)}}d\theta \\ &\quad-\frac{(b^2-a^2)}{b^2(1+a^2)}\underbrace{\int_0^{\pi/2}\frac{\sin^2(\theta)}{\left[1-\frac{(a^2-b^2)}{(1+a^2)}\sin^2(\theta)\right]\sqrt{1-\frac{(b^2-a^2)}{b^2(1+a^2)}\sin^2(\theta)}}d\theta}_{II} \\ &= \Pi\left(\frac{(a^2-b^2)}{(1+a^2)},\frac{(b^2-a^2)}{b^2(1+a^2)}\right)-\frac{(b^2-a^2)}{b^2(1+a^2)}II.\end{aligned}$$

in terms of $a, b, \mathrm{K}$, and $\Pi$. Substituting the new expression of $II$ into $I_1$, and the normalized circumference is now given by

$$\Lambda(a,b) = \frac{2}{\pi b\sqrt{1+a^2}}\left((1+b^2)\Pi\left(\frac{(a^2-b^2)}{(1+a^2)}, \frac{(b^2-a^2)}{b^2(1+a^2)}\right) - \mathrm{K}\left(\frac{(b^2-a^2)}{b^2(1+a^2)}\right)\right).$$

## ACKNOWLEDGMENT

The authors would like to thank L. Salak for editing this paper.

## REFERENCES

[1] P. J. Basser, J. Mattiello, and D. LeBihan, "MR diffusion tensor spectroscopy and imaging," *Biophys. J.*, vol. 66, no. 1, pp. 259–267, Jan. 1994.

[2] P. J. Basser, J. Mattiello, and D. LeBihan, "Estimation of the effective self-diffusion tensor from the NMR spin echo," *J. Magn. Reson., B*, vol. 103, pp. 247–254, Mar. 1994.

[3] C. Pierpaoli and P. J. Basser, "Toward a quantitative assessment of diffusion anisotropy," *Magn. Reson. Med.*, vol. 36, pp. 893–906, Dec. 1996.

[4] C. Pierpaoli, P. Jezzard, P. J. Basser, A. Barnett, and G. D. Chiro, "Diffusion tensor MR imaging of the human brain," *Radiology*, vol. 201, no. 3, pp. 637–648, Dec. 1996.

[5] J. J. Neil, S. I. Shiran, R. C. McKinstry, G. L. Schefft, A. Z. Snyder, C. R. Almli, E. Akbudak, J. A. Aronovitz, J. P. Miller, B. C. Lee, and T. E. Conturo, "Normal brain in human newborns: Apparent diffusion coefficient and diffusion anisotropy measured by using diffusion tensor MR imaging," *Radiology*, vol. 209, pp. 57–66, 1998.

[6] J. S. Shimony, R. McKinstry, E. Akbudak, J. A. Aronovitz, A. Z. Snyder, N. F. Lori, T. S Cull, and T. E. Conturo, "Quantitative diffusion-tensor anisotropy brain MR imaging: Normative human data and anatomical analysis," *Radiology*, vol. 212, pp. 770–784, 1999.

[7] A. L. Alexander, K. Hasan, G. Kindlmann, D. L. Parker, and J. S. Tsuruda, "A geometric analysis of diffusion tensor measurements of the human brain," *Magn. Reson. Med.*, vol. 44, pp. 283–291, 2000.

[8] C. Pierpaoli, A. Barnett, S. Pajevic, R. Chen, L. Penix, A. Virta, and P. Basser, "Water diffusion changes in wallerian degeneration and their dependence on white matter architecture," *NeuroImage*, vol. 13, pp. 1174–1185, Jun. 2001.

[9] P. J. Basser, "Fiber-tractography via diffusion tensor MRI (DT-MRI)," in *Proc. Int. Soc. Magn. Reson. Med.*, 1998.

[10] T. E. Conturo, N. F. Lori, T. S. Cull, E. Akbudak, A. Z. Snyder, J. S. Shimony, R. C. McKinstry, H. Burton, and M. E. Raichle, "Tracking neuronal fiber pathways in the living human brain," *Proc. Nat. Acad. Sci.*, vol. 96, pp. 10422–10427, 1999.

[11] S. Mori, B. J. Crain, V. P. Chacko, and P. C. M. Van Zijl, "Three-dimensional tracking of axonal projections in the brain by magnetic resonance imaging," *Ann. Neurol.*, vol. 45, no. 2, pp. 265–269, 1999.

[12] P. Basser, S. Pajevic, C. Pierpaoli, J. Duda, and A. Aldroubi, "In vivo fiber tractography using DT-MRI data," *Magn. Reson. Med.*, vol. 44, no. 4, pp. 625–632, 2000.

[13] C. Poupon, C. A. Clark, V. Frouin, J. Regis, I. Bloch, D. Le Bihan, and J. F. Mangin, "Regularization of diffusion-based direction maps for the tracking of brain white matter fascicles," *NeuroImage*, vol. 12, pp. 184–195, 2000.

[14] C. Poupon, J. Mangin, C. Clark, V. Frouin, J. Rgis, D. L. Bihan, and I. Bloch, "Towards inference of human brain connectivity from MR diffusion tensor data," *Med. Image Anal.*, vol. 5, no. 1, pp. 1–15, 2001.

[15] S. Pajevic, A. Aldroubi, and P. J. Basser, "A continuous tensor field approximation of discrete DT-MRI data for extracting microstructural and architectural features of tissue," *J. Magn. Reson.*, vol. 154, pp. 85–100, Jan. 2002.

[16] G. J. M. Parker, C. A. M. Wheeler-Kingshott, and G. J. Barker, "Estimating distributed anatomical connectivity using fast marching methods and diffusion tensor imaging," *IEEE Trans. Med. Imag.*, vol. 21, no. 5, pp. 505–512, May 2002.

[17] P. J. Basser, "Quantifying errors in fiber-tract direction and diffusion tensor field maps resulting from MR noise," in *Proc. Int. Soc. Magn. Reson. Med.*, 1997.

[18] P. J. Basser and S. Pajevic, "Statistical artifacts in diffusion tensor MRI (DT-MRI) caused by background noise," *Magn. Reson. Med.*, vol. 44, pp. 41–50, Jul. 2000.

[19] D. Jones, "Determining and visualizing uncertainty in estimates of fiber orientation from diffusion tensor MRI," *Magn. Reson. Med.*, vol. 49, no. 1, pp. 7–12, 2003.

[20] L.-C. Chang, C. G. Koay, C. Pierpaoli, and P. J. Basser, "Variance of estimated dti-derived parameters via first-order perturbation methods," *Magn. Reson. Med.*, vol. 57, no. 1, pp. 141–149, Jan. 2007.

[21] M. Boguna, S. Pajevic, P. J. Basser, and G. H. Weiss, "A model for noise effects on fibre tract trajectories in diffusion tensor imaging: Theory and simulations," *New J. Phys.*, vol. 7, pp. 1–10, 2005.

[22] D. K. Jones, A. R. Travis, G. Eden, C. Pierpaoli, and P. J. Basser, "PASTA: Pointwise assessment of streamline tractography attributes," *Magn. Reson. Med.*, vol. 53, pp. 1462–1467, 2005.

[23] T. E. J. Behrens, M. W. Woolrich, M. Jenkinson, H. Johansen-Berg, R. G. Nunes, S. Clare, P. M. Matthews, J. M. Brady, and S. M. Smith, "Characterization and propagation of uncertainty in diffusion-weighted MR imaging," *Magn. Reson. Med.*, vol. 50, pp. 1077–1088, Nov. 2003.

[24] G. Parker, H. Haroon, and C. Wheeler-Kingshott, "A framework for a streamline-based probabilistic index of connectivity (pico) using a structural interpretation of MRI diffusion measurements," *J. Magn. Reson. Imag.*, vol. 18, no. 2, pp. 242–254, 2003.

[25] C. G. Koay, L.-C. Chang, C. Pierpaoli, and P. J. Basser, "Error propagation framework for diffusion tensor imaging via diffusion tensor representations," *IEEE Trans. Med. Imag.*, vol. 26, no. 8, pp. 1017–1034, Aug. 2007.

[26] H. K. Jeong, Y. Lu, Z. Ding, and A. W. Anderson, "Characterizing cone of uncertainty in diffusion tensor MRI," *Proc. Int. Soc. Magn. Reson. Med.*, 2005.

[27] M. Lazar, J. H. Lee, and A. L. Alexander, "Axial asymmetry of water diffusion in brain white matter," *Magn. Reson. Med.*, vol. 54, pp. 860–867, 2005.

[28] M. Lazar and A. Alexander, "Bootstrap white matter tractography (BOOT-TRAC)," *NeuroImage*, vol. 24, no. 2, pp. 524–532, 2005.

[29] A. W. Anderson, "Theoretical analysis of the effects of noise on diffusion tensor imaging," *Magn. Reson. Med.*, vol. 46, pp. 1174–1188, 2001.

[30] M. Lazar and A. L. Alexander, "An error analysis of white matter tractography methods: Synthetic diffusion tensor field simulations," *NeuroImage*, vol. 20, no. 2, pp. 1140–1153, Oct. 2003.

[31] Y.-C. Wu, A. S. Field, M. K. Chung, B. Badie, and A. L. Alexander, "Quantitative analysis of diffusion tensor orientation: Theoretical framework," *Magn. Reson. Med.*, vol. 52, pp. 1146–1155, 2004.

[32] O. Friman, G. Farnebäck, and C.-F. Westin, "A bayesian approach for stochastic white matter tractography," *IEEE Trans. Med. Imag.*, vol. 25, no. 8, pp. 965–978, Aug. 2006.

[33] G. R. Hext, "The estimation of second-order tensors, with related tests and designs," *Biometrica*, vol. 50, pp. 353–357, 1963.

[34] K. Fukunaga, *Introduction to Statistical Pattern Recognition*. New York: Academic, Mar. 1972.

[35] D. K. Jones and P. J. Basser, "Squashing peanuts and smashing pumpkins: How noise distorts diffusion-weighted MR data," *Magn. Reson. Med.*, vol. 52, no. 5, pp. 979–993, Nov. 2004.

[36] C. G. Koay, J. D. Carew, A. L. Alexander, P. J. Basser, and M. E. Meyerand, "Investigation of anomalous estimates of tensor-derived quantities in diffusion tensor imaging," *Magn. Reson. Med.*, vol. 55, pp. 930–936, 2006.

[37] C. G. Koay, L.-C. Chang, J. D. Carew, C. Pierpaoli, and P. J. Basser, "A unifying theoretical and algorithmic framework for least squares methods of estimation in diffusion tensor imaging," *J. Magn. Reson.*, vol. 182, pp. 115–125, Jul. 2006.

[38] C. G. Koay and P. J. Basser, "Analytically exact correction scheme for signal extraction from noisy magnitude MR signals," *J. Magn. Reson.*, vol. 179, pp. 317–322, 2006.

[39] K. M. Hasan, P. J. Basser, D. L. Parker, and A. L. Alexander, "Analytical computation of the eigenvalues and eigenvectors in DT-MRI," *J. Magn. Reson.*, vol. 152, pp. 41–47, 2001.

[40] D. M. Bates and D. G. Watts, *Nonlinear Regression Analysis and its Applications*. New York: Wiley, 1988.

[41] R. A. Horn and C. R. Johnson, *Topics in Matrix Analysis*. Cambridge, U.K.: Cambridge Univ. Press, 1991.

[42] W. H. Press, S. A. Teukolsky, W. T. Vetterling, and B. P. Flannery, *Numerical Recipes in C*. Cambridge, U.K.: Cambridge Univ. Press, 1992.

[43] T. M. Apostol, *Mathematical Analysis*, 2 ed. Reading, MA: Addison-Wesley, 1974.

[44] H. S. M. Coxeter, *Introduction to Geometry*, 2nd ed. New York: Wiley, 1969.

[45] M. do Carmo, *Differential Geometry of Curves and Surfaces*. Englewood Cliffs, NJ: Prentice-Hall, 1976.

[46] L. M. Milne-Thomson, , M. Abramowitz and I. A. Stegun, Eds., "Elliptical integrals," in *Handbook of Mathematical Functions*. New York: Dover, 1965, pp. 587–628.

[47] "Erratum to Error Propagation Framework for Diffusion Tensor Imaging via Diffusion Tensor Representations," *IEEE Trans. Med. Imag.*, vol. 26, no. 10, p. 1424, Oct. 2007.